Korean J. Chem. Eng., 34(3), 829-843 (2017)
DOI: 10.1007/s11814-016-0302-4

pISSN: 0256-1115
eISSN: 1975-7220

The influence of nanoparticles on gas transport properties of mixed matrix membranes: An experimental investigation and modeling

Mona Jamshidi*, Vahid Pirouzfar,†, Reza Abedini***, and Mona Zamani Pedram******

*Department of Chemical Engineering, Islamic Azad University, Central Tehran Branch, Tehran, Iran
**Young Researchers and Elite Club, Central Tehran Branch, Islamic Azad University, Tehran, Iran
***Faculty of Chemical Engineering, Babol Noshirvani University of Technology, Babol, Iran
****Faculty of Mechanical Engineering-Energy Division, K.N. Toosi University of Technology, Tehran, Iran
(*Received 21 July 2016 • accepted 24 October 2016*)

Abstract−Mixed matrix membranes were made of polysulfone and Matrimid® polymers, and SiO_2 and TiO_2 nanoparticles in order to improve the efficiency of polymeric membrane in gas separation and review the efficiency of membrane separation process, laboratory. The modeling results of selectivity and permeability of gases O_2, N_2, CO_2 and CH_4 were discussed for different membranes. Another objective of this study was to submit a report on the importance of the statistical analysis and modeling in design and optimizing mixed matrix membranes to separate gas. The D-optimal method was applied to model and optimize the selectivity and permeability due to the main parameters. The obtained results indicated that the permeability of all gases demonstrated an ascending trend when the nanoparticles were increased. Under optimized conditions, the permeability of the gases O_2, N_2, CO_2, CH_4 in the membrane of PSF (12)/SiO_2 (13.82) was 2.49, 1.113, 12.82 and 0.885 Barrer, respectively. A statistical method was practiced in the current research to design, optimize and separate gas membranes through effective efficiency for different applications.

Keywords: Mixed Matrix Membranes, Modeling and Optimization, Permeability, Selectivity, D-optimal Design

INTRODUCTION

The importance of gas separation has been verified in different industries and many applications [1,2]. Gas membranes are in intensive competition with other separation methods, such as absorption, adsorption and cryogenics distillation [3]. Membranes have been converted into a developed process due to their simple function and low energy consumption [4]. Among different materials for the preparation of membranes, polymer membranes have been considered the most convenient to separate gas in many processes such as air purification [5]. Low permeability and selectivity of a polymer membrane have been identified as the most prominent problem directed into some limitations in the industrial application of these membranes [6-8]. Different methods have been put into practice to overcome such limitations. Moreover, making mixed network membranes is one effort to increase the efficiency and improve the properties of polymer membrane for gas separations. In this method, a balance between permeability and selectivity can be provided by inorganic fillers through an organic polymer network [9,10]. Meanwhile, some properties can be achieved which cannot be found in a pure polymer membrane. Within the last two decades, glassy polymers have been widely applied in gas separation due to their excellent heat, chemical stability and great selectivity. These polymers transmit small gas molecules at higher speeds, in comparison to large molecules [11,12].

Among the glassy polymers, polyimides [13-17], polycarbonates [18], polysulfones [19-23] and polypyrrolones [24] and others are used as high performance membranes. However, the low performance of these polymers has caused some limitations in the industrial applications.

Polysulfone is a widely used polymer with fairly suitable chemical and thermal stability at severe temperature and high pressure conditions. The selectivity of this polymer against small gas molecules, such as hydrogen and oxygen, is more than that of methane and nitrogen. Adding silica nanoparticles to polysulfone is one possible option to improve membrane efficiency. Guiver et al. studied the effect of adding silica to polysulfone and observed that permeability values of methane, nitrogen, hydrogen and carbon dioxide gases increased up to 370, 400, 170 and 212% in comparison with the pure polysulfone for a distribution of 20 vol% of silica nanoparticles [23].

In another research, adding silica nanoparticles to PMP membrane made normal permeability of butane in a membrane containing 45 wt% of particles increased four-times in comparison to that of pure polymers. Similarly, the presence of the silica nanoparticles increased the permeability and selectivity of butane in AF2000 polymer [25,26].

Matteucci et al. [26] studied the permeability of CO_2, N_2 and CH_4 by adding TiO_2 nanoparticles to PTMSP polymer. When nanoparticles were loaded in a high range, the permeability of these gases increased four-times more than the pure polymer. They scrutinized the effect of TiO_2 nanoparticles to PB polymer in another research. The results indicated that the permeability of the coefficients of CO_2, CH_4, N_2 and H_2 gases increased three-times more than the initial

†To whom correspondence should be addressed.
E-mail: v.pirouzfar@iauctb.ac.ir

values in a membrane containing 27 vol% TiO_2 nanoparticles. The solubility coefficient of the gases was enhanced by adding nanoparticles in this experiment, while the permeability coefficients decreased by adding the nanoparticles.

Moghaddam et al. [27] analyzed the effect of TiO_2 particles based on the Matrimid® polymer. The permeability of N_2, CH_4, and CO_2 was measured to determine the effect of TiO_2 on the efficiency of the Matrimid membrane. For example, the permeability of N_2, CH_4 and CO_2 increased 2.76, 3.3 and 1.86 times than those of the pure Matrimid. In fact, these results demonstrated that using TiO_2 nanoparticles improved the efficiency of the membrane to separate CO_2/CH_4.

Experimental design and statistical modeling can be effectively employed to determine and prove the relationship between multi parameters and a set of experimental parameters in the field of membrane preparation and application [28,29]. Many researchers utilized a statistical method to evaluate the effect of various variables including concentration of the polymer and its additives in casting solutions, solvent evaporation time and coagulation bath temperature on both structural characteristics of the membranes and performance of the polymeric membranes [30,31].

Khayet et al. [32] utilized a statistical method to assess the influence of various variables including concentration of the polymer and its additives (polyethylene glycol, PEG) in casting solutions, solvent evaporation time and coagulation bath temperature on both structural characteristics of the membranes and performance of the polymeric membranes. The analysis of variance showed that all variables had significant effects on the responses. The coagulation bath temperature played the least important role, while the concentration of PVDF-HFP had the greatest effects on both permeate flux and salt rejection coefficient. Onsekizoglu et al. [33] used a two-level factorial experimental design to study the influence of main operating parameters on the evaporation flux and soluble solid content of apple juice during concentration through osmotic distillation (OD) and membrane distillation (MD) processes. The factorial models were obtained from experimental design to investigate all interactions between the analyzed parameters (osmotic agent concentration, flow rate and temperature difference between feed and osmotic agent), and these models were validated statistically by analysis of variance (ANOVA). Models were developed to estimate the evaporation flux and soluble solid influenced by operating analyzed variables in this system. Results have revealed that all the linear terms of the factors have significant effects on the evaporation flux.

Su et al. [34] applied statistical two-level factorial design to evaluate the effect of various pyrolysis parameters on the performance of the membranes prepared from Kapton® 100HN polyimide. The effects of the carbonization atmosphere, final temperature, heating rate and the thermal soaking time were examined at the final temperature on the permeation rates of He, CO_2, O_2 and N_2. Statistically speaking, significant carbonization parameters including main factors and two-factor interactions of the selected factors were studied by analyzing the probability values. Results disclosed that the carbonization temperature was the controlling parameter determining the transport properties of the membranes.

On the other hand, statistical analysis and modeling were applied in one previous study to examine the design and optimization of the membranes for gas separation. A factorial methodology was employed to optimize the permeability and selectivity. This was done through implementing the general factorial design considering three main variables selected by the precursor materials (Matrimid, P84 and Torlon), blend composition and final pyrolysis temperature (600, 700 and 800 °C). Findings taken from statistical analysis demonstrated that linear and quadric terms of these three factors caused significant effects. The optimal conditions obtained from Matrimid, blend composition of 70%, and pyrolysis temperature of 800 °C. Due to these conditions, the model estimated the selectivity values of 120.2, 8.39 and 8.06 for CO_2/CH_4, H_2/CO_2 and O_2/N_2, respectively [35].

According to the above-mentioned explanations about the parameters affecting the membrane properties and the complexities involved in the preparation of high performance membranes, our main objective was to study the effects of different polymers (Matrimid® and polysulfone). Another objective was to investigate the percentage of the polymer used to evaluate the effect of nanoparticle type (TiO_2 and SiO_2) and their percentage to improve the gas permeation and separation performance in the mixed matrix membranes. Another aim was to use factorial design to identify the effects of the experimental variables to reach optimal conditions for high performance mixed matrix membranes made from Matrimid® and polysulfone. These membranes demonstrate various molecular structures and are prepared by various mixing procedures of nanoparticles. To the best of our knowledge, this is the first study on the modeling the mixed matrix membranes derived from polymeric blend precursors. Therefore, the results obtained from this research can shed light for further developments in further exploitation of blend membranes for diverse separation applications. In this work, in addition to being a new membrane made for experimental investigations of developed MMMs with objectivity for different applications. The new modeling and optimizing procedures have been followed as new procedures for future works. Some of the developed membranes perfectly surpass the upper bound. However, the key value adding our research to this subject is that we are have offered a statistical technique and applied it to demonstrate that researchers can rely on it for development of much better membranes for any desirable application. By applying these models, different values of gas permeability and gas pair selectivity can be obtained in different percentages of both polymers (Matrimid® and Polysulfone) and nanoparticles (TiO_2 and SiO_2). In addition to the listed polymers and nanoparticles, these models have a good approximation for the same polymers and nanoparticles to predict the mentioned response for gas transport properties. The permeability and selectivity of CH_4, N_2, O_2 and CO_2 gases have been studied to investigate the specifications in these membranes. These experiments were also optimized and modeled for the industrial applications in gas separation.

EXPERIMENTAL TECHNIQUES AND METHODOLOGY

1. Materials

The materials used in this research, including Matrimid® (Poly

Table 1. Physical properties of TiO_2 and SiO_2 nanoparticles

Typical properties	(TiO_2)	(SiO_2)
Specific surface area (BET)	500 m^2/g	200 m^2/g
Bulk density	0.6 g/cc	0.048 g/cc
True density	3.7 g/cc	1.24 g/cc
Moisture content	≤4%	0.02
Ti and Si content (based on metal)	>99.999%	>99.8%

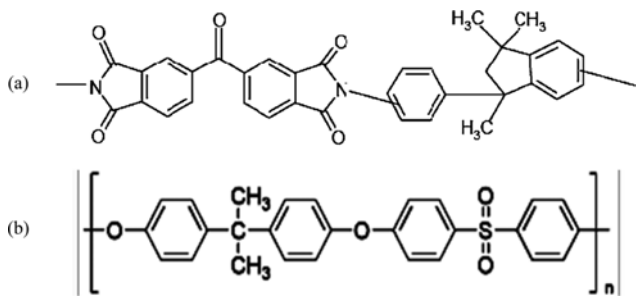

Fig. 1. Chemical structure of (a) Matrimid® (b) polysulfone.

[3,3′,4,4′-benzophenone tetracarboxylic dianhydride and 5(6)-amino-1-(4-aminophenyl-1,3-trimethylindane)], BTDA-DAPI), were purchased from Hunstman LLC corporation, and polysulfone supplied from Aldrich Chemical Company Inc. (Milwaukee, USA). The nanoparticles of titanium dioxide (TiO_2) and fumed silica (SiO_2) were supplied from nanoscale (Manhattan, KS) and PlasmaChem (Berlin, Germany), respectively. The physical properties of TiO_2 and SiO_2 nanoparticles are reported in Table 1, while the chemical structures of Matrimid® and Polysulfone are shown in Fig. 1.

2. Characterization Techniques

To study morphology of the mixed matrix membrane, pure matrimid, matrimid/SiO_2 and PSF/TiO_2 MMMs were analyzed by scanning electron microscopy (SEM). The results of thermal decomposition of some membranes and weight stability of pure polymer were analyzed by TGA. Then, the obtained results were compared to those of MMM. In this study, we monitored the thermal properties of the polymeric membrane and MMM through differential scanning calorimetry (DSC) using a Rheometric Scientific with Ar purging at a flow rate of 30 $mL \cdot min^{-1}$. The applied temperature range was from 25 to 700 °C. A wide-angle X-ray diffraction (WAXD) was employed to verify microstructural characteristics of the membranes. Measurements used an STOE Model Stadi MP (STOE, Germany) at room temperature. A standard displacement technique was used to calculate the density of films [36]. The fractional-free volume (FFV) of polymer and MMMs were calculated by the Bondi group contribution method [37].

3. Preparation of Polymeric and MMMs

Mixed matrix membranes derived from Matrimid® and polysulfone polymeric precursors were filled by TiO_2 and SiO_2 nanoparticles and prepared as dense films by solution-casting method. Initially, the dried polymer powders were gradually dispersed and dissolved in a hot NMP (150 °C) while stirring by a magnetic stirrer under purging an inert nitrogen gas. It took about 8 h to reach complete dissolution. At the next step, nanoparticle powders of TiO_2 and SiO_2 were added and dispersed in the polymeric solution while stirring continuously at 150 °C for another 6 h to allow a thorough homogenization of the blend components. Before adding nanoparticle to the solution, they were sonicated for 10 min to get a homogeneous solution. Finally, the subsequent solutions were filtered through a 0.2 μm filter to remove any dust particle and non-dissolved material. After degassing, polymeric solutions were poured into a Pyrex glass and casted using a film applicator. While cast on the Pyrex, the films were placed inside an oven. For slow evaporation of NMP, a temperature protocol was adjusted in the following order: 24 h in 70 °C, 24 h in 80 °C, and 24 h in 100 °C. Keeping under vacuum, the temperature of the oven was progressively raised at the rate of 40 °C/h to the final temperature of 160 °C. The mixed matrix membranes were also kept at this final temperature for 1 hour to ensure complete removal of the residual solvents. The dried membranes were finally collected after natural cooling. The solution concentration of 12 wt% was selected to prevent nanoparticle sedimentation at lower concentration. On the other hand, it was detected that nanoparticle dispersion (more than 18 wt%) affects aggregate formation on the top surface of the MMMs at high concentration. So, the polymeric powder added in the NMP at 12 and 18 wt%. The nanoparticles were also added to this polymeric solution at 5, 10 and 15 wt%, with thickness of the fabricated membranes being 60 μm. The gas permeability for the mixed matrix membranes was measured accordingly for CH_4, N_2, O_2 and CO_2 through the following equation:

$$P = \frac{273.15 \times 10^{10} vl}{760 AT((p_0 \times 76)/14.7)}\left(\frac{dp}{dt}\right) \quad (1)$$

where, P is the gas permeability of the mixed matrix membrane in Barrer; A refers to the area of the membrane (cm^2); T stands for the operating temperature (K); and the feed gas pressure in the up-stream is given by P_0 (Psi); V denotes the volume of the down-stream (cm^3) which is selected to be the same in the permeability test for all the membranes, and finally, l represents the membrane thickness (cm). An ideal selectivity of gas A to gas B is defined as follows:

$$\alpha_{A/B} = \frac{P_A}{P_B} \quad (2)$$

where, P_A and P_B are the permeability values of the pure gases A and B (barrer), respectively. The permeability tests were conducted at 10 atm and 35 °C.

4. Statistical Analysis and Model Development

Factorial is an efficient tool to design of experiments, model and evaluate the effects of different variables and find the optimized conditions to get a response. For this purpose, a method consisting of factorial was applied to design of the experiments and statistical analysis to provide an effective model. Compared to statistical access, the principal preference of the factorial design is the possibility of synthesis in such a way that the interactions between all variables are considered. For statistical calculations, experimental variables of X_{actual} in the frame of X_{coded} were coded on the basis of the following equation:

$$X_{coded} = \frac{X_{actual} - \overline{X}}{d} \quad (3)$$

X_{coded} is the coded (dimensionless) amount of the variables (X_{actual}), is the average amount (X_{actual}) and "d" gives the difference between $\overline{X}$ and X_{actual}.

The responses may be written as the function of variables with multiple regression applications using the least square method, proportional to the following relation:

$$Y=b_0+b_1X_1+b_2X_2+b_3X_3+b_4X_4+b_{12}X_1X_2+b_{13}X_1X_3+\ldots \quad (4)$$

In Eq. (4), b_0 is a general coefficient; b_i denotes the coefficient of linear effects and b_{ij} denotes the coefficient of quadratic effects. X_1, X_2, X_3 and X_4 are the model variables. Different combinations of the parameters or variables (e.g., X_1X_2) address an interaction between the individual parameters. The regression procedure was carried out in the coded units and the actual equation was obtained from derivation of the coded equation. With respect to the process, when using the ploy-nominal equations is necessary for modeling, the encoding method enables execution of the same.

In this study, a general factorial with D-optimal design was employed to model the gas permeability and selectivity in the mixed matrix membranes since type of the polymer (X_1), percentage of the polymer (X_2), type of the nanoparticle (X_3) and percentage of the nanoparticle (X_4) were chosen as the independent variables. One of the major advantages of this experimental design method is that it is able to examine all possible interactions and combinations of the levels across current variables in comparison to the conventional and classic statistical approach. Furthermore, the permeability of CH_4 (P_{CH_4}), N_2 (P_{N_2}), O_2 (P_{O_2}) and CO_2 (P_{CO_2}), as well as selectivity of N_2/CH_4 (α_{O_2/N_2}), CO_2/CH_4 (α_{CO_2/CH_4}), O_2/N_2 selectivity (α_{O_2/N_2}) and CO_2/N_2 (α_{CO_2/N_2}), were taken as the responses of the function. Four important variables applied in this analysis are listed in Table 2 with introduction of their relevant types and levels. The variables of polymer type and nanoparticle type are dimensionless (constant and definite).

Table 2. General factorial design matrix of tests with respective variables and levels

Variable	Type	Level	
		Actual	Coded
Type of polymer	X_1	Matrimid	{−1}
		Polysulfone	{1}
Percentage of polymer	X_2	12	−1
		18	1
Type of nano particle	X_3	TiO_2	{−1}
		SiO_2	{1}
Percentage of nano particle	X_4	5	−1
		10	0
		15	1

The software package of Design-Expert (Version 7.0.0, 2005; Stat-Ease, Minneapolis, MN, USA) was used for data regression analysis and assessment of the equation coefficients. Meanwhile, canonical analysis was fulfilled to predict formation of the curve produced by the model. The best polynomial model was extracted on the basis of significant amounts ($p<0.05$), coefficient of variation (CV), multiple correlation coefficient (R^2), and appointed multiple correlation coefficient (appointed R^2) which are obtained all from

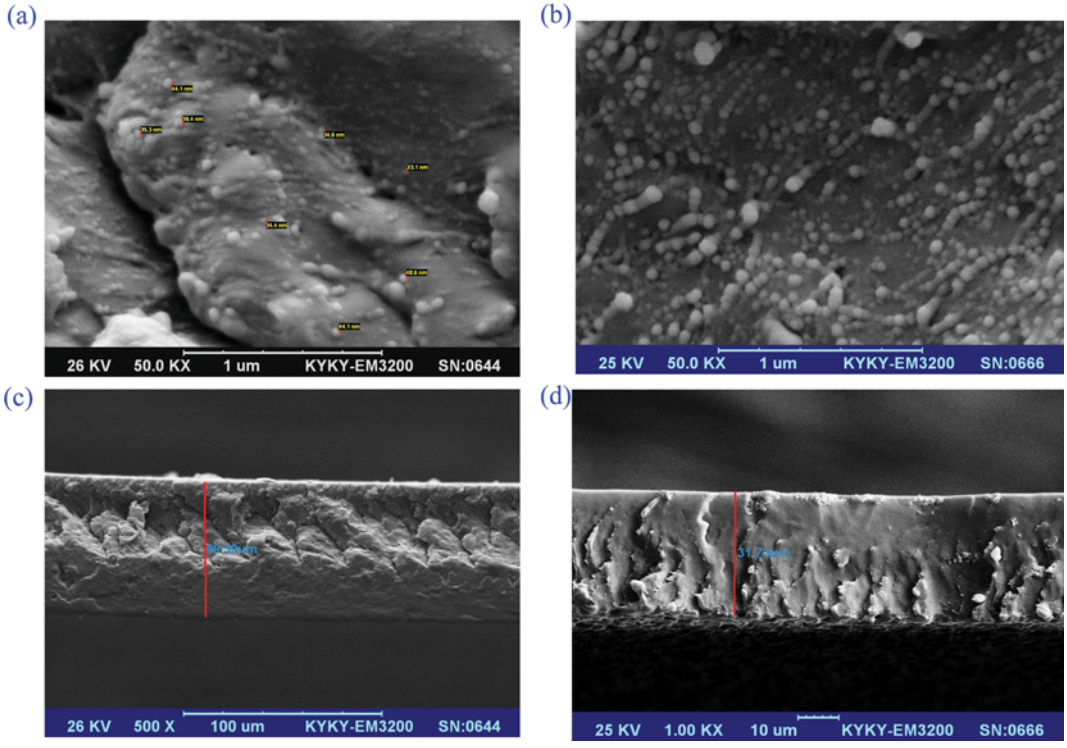

Fig. 2. SEM images of top view of (a) Matrimid/SiO_2 MMM (5 wt% of TiO_2), (b) matrimid/SiO_2 MMM (15 wt% of TiO_2) and cross-sectional view of (c) matrimid/SiO_2 MMM (5 wt% of TiO_2), (d) matrimid/SiO_2 MMM (15 wt% of TiO_2).

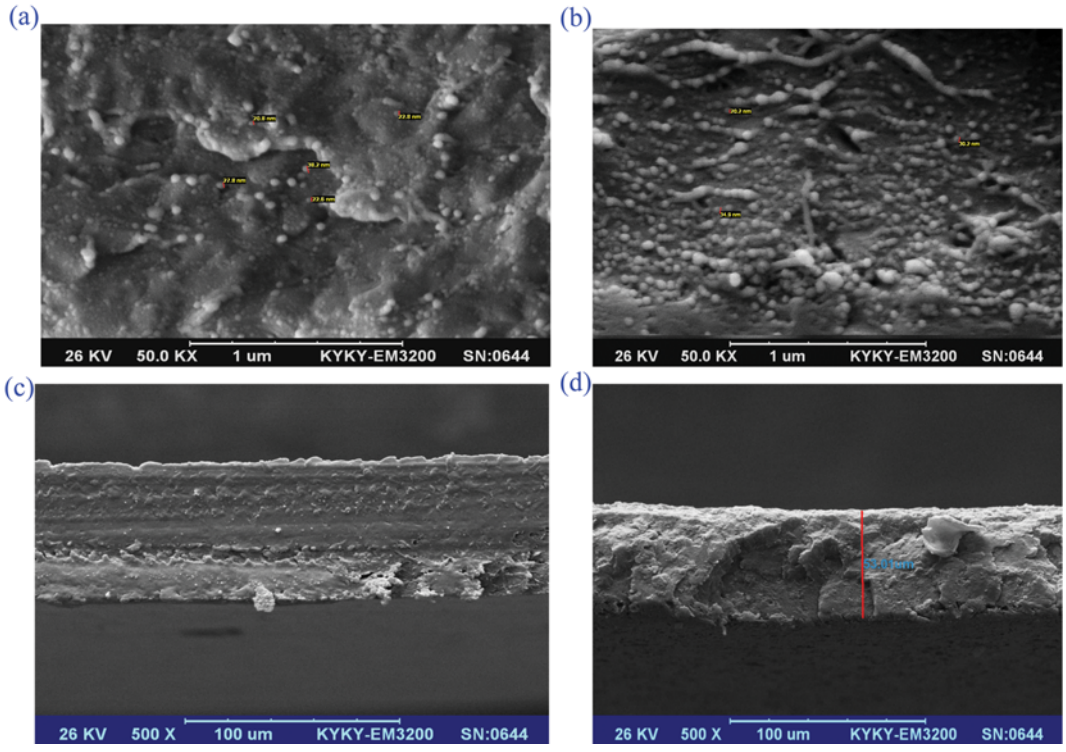

Fig. 3. SEM images of top view of (a) PSF/TiO_2 MMM (5 wt% of TiO_2), (b) PSF/TiO_2 MMM (15 wt% of TiO_2) and cross-sectional view of (d) PSF/TiO_2 MMM (5 wt% of TiO_2), (b) PSF/TiO_2 MMM (15 wt% of TiO_2).

the Design-Expert.

RESULTS AND DISCUSSION

1. Mixed Matrix Membranes Morphology

The morphology of the dispersed phase affects gas permeation and separation performance in the mixed matrix membranes significantly. Figs. 2 and 3 show the SEM micrographs of the top surface and cross-section of a Matrimid/SiO_2 MMM (5 wt% of SiO_2) (Figs. 2(a) and 2(c)) and Matrimid/SiO_2 MMM (5 wt% of SiO_2) (Figs. 2(b) and 2(d)), and also PSF/TiO_2 MMM (5 wt% of TiO_2) (Figs. 3(a) and 3(c)) PSF/TiO_2 MMM (15 wt% of TiO_2) (Figs. 3(b) and 3(d)), respectively. According to Fig. 2, the MMM derived 5 wt% of SiO_2 exhibited a homogeneous morphology, while the MMM composed form Matrimid/SiO_2 (15 wt% of SiO_2) demonstrated inorganic particles dispersed uniformly through the membrane matrix. It seemed that among the two types of MMMs, the Matrimid/SiO_2 matrix membrane incorporated relatively dense homogeneous structures. The SEM images confirmed that the voids between the polymer chains and the filler particles were heavily dependent on concentration of the inorganic fillers. From the cross-sectional images, it can be observed that the membranes become more porous with nanoparticle dispersion. Also, it can be found that the nanoparticles avoid membrane chains to approach closer. Thus, free volume is also created.

Table 3 presents the fraction of free volume, glass transition temperature (Tg) and physical properties of polymer and mixed matrix membranes. It is recognized that the Tg of the polymeric membranes will be enhanced by raising the nanoparticles loading onto the mixed matrix membranes. Data in this table indicate that polymer membrane possess lower fractional free volumes. The diversity in FFV of these polymers possibly stems to be the type of chemical structure. It seems that adding nanoparticles slightly increases the density of the MMMs. However, further increasing of nanoparticle loading reduces the density of developed membranes. This may be due to the agglomeration impact of the nanoparticles started to occur at upper loading percentages. These density analysis results can be applied for evaluating the FFV that probably affected by the weak interaction between the nanoparticles and the polymer chain network. Generally, gas transport properties in MMMs depends on membrane's structure. In addition, membrane's structure significantly relies on the interface between nanoparticle and polymer. As nanoparticles get increased in these membranes, the permeability increased on interface between nanoparticle and polymer. Some of chain packing gets connected to the surface of nanoparticle and caused free volume is created on the interface. In fact, the

Table 3. The physical properties and fraction of free volume for polymer and mixed matrix membranes

Sample	Density (g/cm^3)	FFV	Tg (^oC)
Pure matrimid	1.17	0.268	323.1
Pure PSF	1.24	0.156	187
PSF/TiO_2 MMM (5 wt% of TiO_2)	1.21	0.171	189.6
PSF/TiO_2 MMM (10 wt% of TiO_2)	1.14	0.185	193.3
Matrimid/SiO_2 MMM (15 wt% of SiO_2)	1.10	0.295	335.4

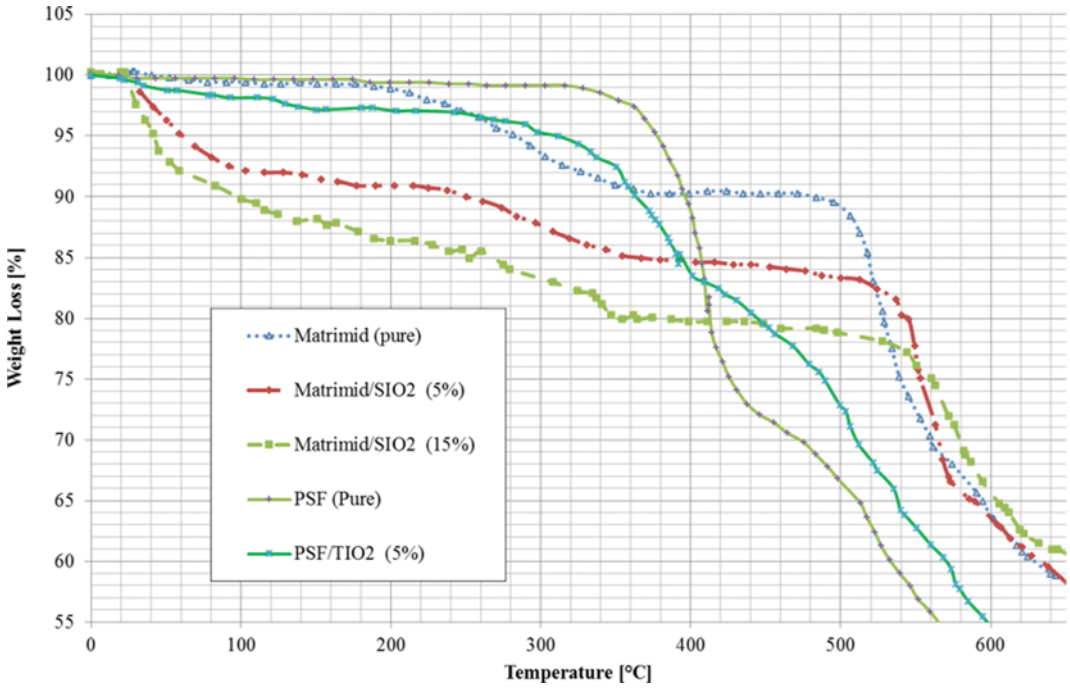

Fig. 4. The results of the TGA carried out on membranes applying constant temperature protocols (10 °C/min). Weight loss [%] versus temperature.

free volume will be increased. The repulsive force between polymer and filler particles is also regarded as another reason forming free volume on interface.

2. Thermal Stability of Membranes and XRD Characteristics

TGA is one of the most widely applied techniques determining the weight loss of each membrane as a function of temperature. This measurement was performed on the MMM samples with different nanoparticle loading. We can also specify the influence of nanoparticle loading onto the thermal stability of the developed membranes by implementing this analysis. Fig. 4 depicts the TGA results for various membrane composed of Matrimid and PSF with nanoparticles using a constant temperature increment rate (e.g., 10 °C/min) under a nitrogen atmosphere. In this figure, thermal gravimetric analysis is addressed for the pure Matrimid and PSF and three types of MMM, namely a Matrimid/SiO_2 membranes, containing 5 wt% of SiO_2 nanoparticles, a Matrimid/SiO_2 membranes containing 15 wt% of SiO_2 Nanoparticles, and a PSF/TiO_2 membrane with 5 wt% of TiO_2 nanoparticles. Weight loss in the pure PSF sample started at about 325 °C and pure Matrimid about 180 °C. Thermal degradation was remarkable between 300 and 450 °C. At 550 °C, 28 wt% of the pure Matrimid and 43 wt% of PSF remained. At this temperature, weight percentages of the residual material were found to be approximately 78, 63 and 76 for Matrimid/SiO_2 (5 wt%), PSF/SiO_2 (5 wt%), PSF/SiO_2 (5 wt%) and Matrimid/SiO_2 (15 wt%), respectively. The obtained results showed that the membranes with higher content of the modified nanoparticles incorporate greater weight loss at lower temperatures, while this trend was vice versa at high temperatures. These results might be achieved from the enhancing formation of free volume and voids between the nanoparticles surface and polymer chain. Moreover, the TGA results indicated that no residual solvent was present in the membranes. Same as our results, Lua et al. [38] in their study reported the TGA test on the membrane. The decomposition of Kapton 100HN begins around 773 K and the sample weight decreases significantly within a narrow temperature range of 773-923 K. at the final temperature (1,123 K) amount of residues was about 55% of the starting weight. In another research, Pei Shi Tin et al. [39] illustrate the weight variation of polymer during the heating process from 50 to 900 °C. The total weight loss at 800 °C for P84 was approximately 51%. Briefly, P84 started decomposes evidently at around 500 °C. The XRD spectra as a function of the degree of crystallinity or amorphousness were obtained for further structural characterization of the mix matrix membranes as shown in Fig. 5. The results obtained for the Matrimid pure and Matrimid/SiO_2 in 5 and 15 wt% samples are indicated in this figure. The XRD patterns of the crystalline membranes shows sharp peaks, while that of the amorphous membranes indicate a single broad diffused peak. There is no evident variation in both the intensity and position of the patterns of pure Matrimid and Matrimid/SiO_2, which proposes that nanoparticles of SiO_2 do not affect the Matrimid precursors network d-spacing. Similarly, Lua et al. [38] submitted the XRD spectrum of the Kapton film that gives three peaks at 2θ=15.10°, 22.44° and 26.12° with the most intense peak appearing at 2θ= 22.44°. Also, in Hosseini et al. [40] the XRD pattern for membrane carbonized at 600 °C is a merger of two amorphous peaks appeared at 22.7° and 25.4° and another peak located at 2θ=45.1°.

3. Regression Models for Response

Different experimental conditions and response of the gases to the different amounts of variables are briefly mentioned in Table 4. As shown, the permeability results of the pure gases indicate an increment in the gas permeability in comparison to the volume-fraction of added nanoparticles. However, the amount of this incre-

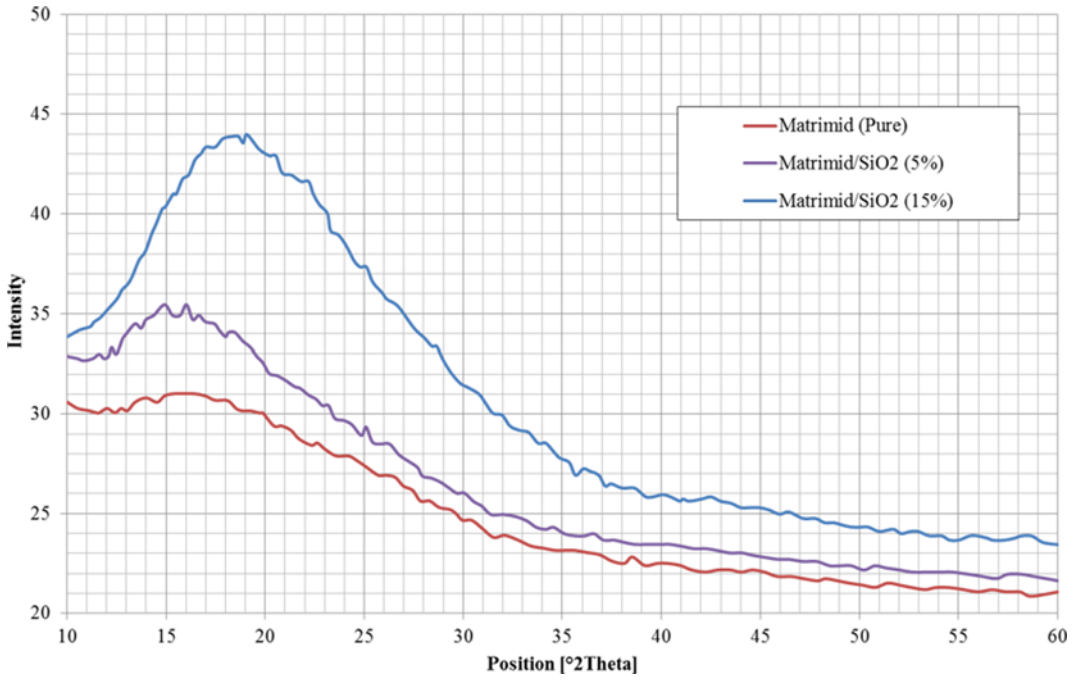

Fig. 5. The effect of variations in the nano-particle percentage on the microstructure of mixed matrix membranes evaluated by X-ray diffraction analysis.

Table 4. The experimental values of gas permeability and ideal selectivity

Run	Variable				Response							
					Permeability (barrer)				Selectivity			
	X_1	X_2	X_3	X_4	P_{CH_4}	P_{N_2}	P_{O_2}	P_{CO_2}	α_{N_2/CH_4}	α_{CO_2/CH_4}	α_{O_2/N_2}	α_{CO_2/N_2}
1	Matrimid	12	TiO_2	5	0.37	0.41	1.89	6.4	1.125	17.41	4.58	15.47
2			TiO_2	10	0.48	0.58	2.00	8.5	1.220	17.67	3.43	14.49
3			TiO_2	15	0.62	0.79	1.93	10.9	1.276	17.61	2.44	13.80
4			SiO_2	5	0.39	0.43	1.97	6.9	1.101	17.60	4.54	15.98
5		18	TiO_2	5	0.31	0.35	1.57	5.3	1.125	16.88	4.44	15.00
6			TiO_2	10	0.40	0.49	1.72	7.3	1.220	18.05	3.50	14.80
7			TiO_2	15	0.57	0.73	1.82	10.3	1.276	18.10	2.51	14.19
8			SiO_2	5	0.32	0.38	1.65	5.4	1.173	16.70	4.35	14.23
9			SiO_2	10	0.43	0.54	1.85	7.9	1.252	18.38	3.45	14.69
10			SiO_2	15	0.59	0.79	1.99	11.1	1.341	18.96	2.54	14.14
11	Polysulfone	12	TiO_2	5	0.43	0.48	2.19	7.4	1.112	17.30	4.51	15.41
12			TiO_2	15	0.75	0.89	2.28	12.8	1.187	17.07	2.56	14.38
13			SiO_2	5	0.55	0.62	2.06	7.0	1.125	12.68	3.34	11.27
14			SiO_2	10	0.73	0.88	2.41	10.2	1.220	14.05	2.73	11.52
15			SiO_2	15	0.95	1.21	2.45	13.8	1.276	14.54	2.02	11.39
16		18	TiO_2	5	0.45	0.50	1.59	5.6	1.102	12.29	3.20	11.16
17			TiO_2	10	0.56	0.68	1.90	7.6	1.216	13.61	2.79	11.19
18			TiO_2	15	0.84	1.05	2.20	12.7	1.253	15.13	2.09	12.07
19			SiO_2	5	0.47	0.53	1.71	5.8	1.125	12.29	3.24	10.93
20			SiO_2	15	0.87	1.11	2.31	13.0	1.276	14.94	2.07	11.71

ment in the gas permeability is different because specifications of the gases, for example size and solubility of the molecules are different from each other. Consequently, the permeability of the gas molecules with smaller kinetics diameter has been greater than that of the larger molecules because permeability is the dominant parameter in the polyimide membranes and synthetic network. Per-

meability in these membranes scores the maximum value for CO_2 and after that O_2 has the second great permeability.

In terms of efficiency of the polymeric membrane type, the experimental data indicate that the gases under study in the existing experimental conditions have provided the maximum permeability in polysulfone membrane and the maximum selectivity in Matrimid® synthetic membrane. Therefore, it can be observed that changing the polymer type is more effective to improve the gas permeability and selectivity. This clearly shows the effect of compatibility between nanoparticles and polymer in the synthetic network membrane.

The maximum values of permeability for O_2, N_2, CO_2 and CH_4 are equal to 2.45, 1.22, 13.8 and 0.95 Barrer in polysulfone membrane, respectively. Meanwhile, the maximum selectivity for N_2/CH_4, CO_2/CH_4, O_2/N_2 and CO_2/N_2 in the Matrimid® membrane are reported as 1.341, 18.96, 4.58 and 15.98, respectively. The gas selectivity in the mixed matrix membrane has been decreased in comparison to that of the pure polymeric membranes. One possible reason for this reduction may be the partial changes in the nature of the membrane separation process, from the state of being selector based on molecule size, to the state of being selector based on solubility due to the existence of some non-selective holes in the membrane network. For this reason, the holes formed in the network will degrade molecular screen specifications of the membrane which can lead to reduction of the selectivity.

In comparison to the other membranes, the Matrimid/TiO_2 membrane has the maximum selectivity for O_2/N_2 and CO_2/N_2, while the selectivity of N_2/CH_4 and CO_2/CH_4 has reached a greater amount in the Matrimid/SiO_2 synthetic membrane as compared to other membranes. This finding may be in connection with the difference in the micro-structural specifications. The polysulfone/SiO_2 mixed matrix membrane has obtained maximum permeability than other types. Holistically, the permeability of the synthetic network membrane will be increased through the presence of the nanoparticles in the polymer network,in comparison to that of the pure polymer due to smaller compression in polymer chains, increment of free volume in network, variable amounts of gas solubility in polymer network, and formation of holes on interface of nanoparticles and polymer. Remarkably, these changes in the structure of the polymer network arise from the effects of contact between the two organic and inorganic phases.

On the basis of the results obtained from the experiments and multiple regression, the main third-order polynomial equations have been explained and the data have coped with the related equations in different levels and variables. Statistical significance of the proposed models was checked through F-value and p-value. Analysis of variance (ANOVA) for a quadratic model of permeability (for example P_{CO_2}), and the least-square adjustment and variables are shown in Tables 5 and 6.

Table 5. The results of the analysis of variance for the response surface CO_2 permeability model

Model	Sum of squares	Degree of freedom	Mean square	F-value	p-Value Prob>F	Status
Mean vs. total	1545.4	1	1545.4			
Linear vs mean	146.0	4	36.5	99.5	<0.0001	Suggested
2FI vs linear	2.6	6	0.4	1.4	0.3175	
Quadratic vs 2FI	0.7	1	0.7	2.6	0.1467	Aliased
Cubic vs quadratic	1.6	7	0.2	0.4	0.8463	Aliased
Residual	0.6	1	0.6			
Total	1696.9	20	84.8			

Table 6. The least-square fit and parameters (for the CO_2 permeability response)

Source	Sum of squares	Degree of freedom	Mean square	F-value	p-Value Prob>F	Status
Model	149.3	10.0	14.9	60.8	<0.0001	Significant
X_1	4.9	1.0	4.9	19.9	0.0016	
X_2	5.1	1.0	5.1	20.8	0.0014	
X_3	2.2	1.0	2.2	8.8	0.0156	
X_4	127.6	1.0	127.6	519.7	<0.0001	
X_1X_4	1.4	1.0	1.4	5.8	0.0397	
X_2X_3	0.0	1.0	0.0	0.1	0.8212	
X_2X_4	0.3	1.0	0.3	1.1	0.3187	
X_3X_4	0.2	1.0	0.2	0.6	0.4521	
X_4^2	0.8	1.0	0.8	3.4	0.0993	
$X_1X_2X_4$	0.1	1.0	0.1	0.6	0.4762	
Residual	2.2	9.0	0.2			
Cor total	151.5	19				

In accordance with these tables, the total amount of squares and freedom degree (DOF) indicate the overall deviation from the average of each model in addition to the numbers of the terms added to the model. The remainder amounts indicate the remainder DOF. Meanwhile, the average square is the total square divided by DOF (for each Model) and can be used to calculate F-value in the proposed models. The F-value is used to verify the test significance by adding a new term of the model. As an example, the significance of the linear terms was examined upon omitting average and blocks effects. Thereafter, upon omission of average, block and linear effects, significance of quadratic terms was controlled. Cubic models can be found significant based on the amounts summarized in Tables 5 and 6 that have been proposed using the F-value and the minimum probability.

The following models have been proposed for CO_2 permeability and CO_2/CH_4 selectivity after controlling of the statistical significance and using the Multiple Regression Analysis:

$$P_{CO_2}=8.58+0.6\,X_1-0.53X_2+0.34\,X_3+3.02\,X_4+0.32\,X_1X_4 -0.031\,X_2X_3+0.16X_2X_4+0.12\,X_3X_4+0.51\,X_4^2+0.11\,X_1X_2X_4 \quad (5)$$

$$\alpha_{CO_2/CH_4}=16.21-0.88\,X_1-1.38\,X_2+2.17\,X_3+0.11X_4-0.93\,X_1X_3 -0.97\,X_1X_4+0.46\,X_2X_4+0.69X_1X_3X_4-0.98X_2X_3X_4 +1.44X_1X_4^2+1.23X_2X_4^2-1.13X_3X_4^2 \quad (6)$$

Using the analytical procedures and techniques from different second- and third-order, polynomial models were obtained for the permeability of CH_4, O_2 and N_2, as well as the selectivity of N_2/CH_4, O_2/N_2 and CO_2/N_2 as shown in Table 7 with corresponding coded amounts of variables, which are summarized in Table 2. The suggested models reveal that the quadratic and cubic equations have been significant and successfully used to improve the analysis. The minimum P-value is associated with the maximum amount of significance, while the P-value verifies reliability and validity of the model. The related results showed that all the linear, quadratic and cubic variables have significant effect.

The developed models and equations provided in Table 7 with variable estimations and their corresponding p-values suggest that among the independent variables, X_2X_4 and X_2X_4 play not much important role in the permeability of CH_4. The positive coefficients of X_1, X_3 and X_4 imply a linear effect upon increasing the permeability of CH_4, while the negative coefficient of X_2 impose a linear effect on the reduction of the CH_4 permeability. However, the interactions between X_1 and X_4 variables and also X_2 and X_3 variables were effective and significant. In the case of O_2/N_2 selectivity, $X_2X_4^2$ and $X_3X_4^2$ were found as significant terms of the model. Furthermore, based on the selectivity model of CO_2/N_2, X_4^3 was found as a significant term of the model.

4. Comparison between Observed and Estimated Responses

The models of gas transport properties may be used in accordance with the determined amounts of variables to estimate for each one of the responses (e.g., P_{CH_4}, P_{O_2}, P_{N_2}, P_{CO_2}, α_{CO_2/CH_4}, α_{N_2/CH_4}, α_{CO_2/N_2} and α_{O_2/N_2}). This evaluation is usually applied in those data which are located just at the boundaries of analysis so that an extrapolation out of this boundary must be fulfilled accurately. Fig. 6 illustrates a fine conformity between the data obtained from the experimental amounts and those estimated from the gas transport models for both permeability of CO_2 and selectivity of CO_2/CH_4 in the optimized conditions. 3D surface plots for the separation models and gas transport have been shown in in Figs. 7-9 and provide a better arrangement of the effects of different variables. For example, an elliptical figure may result upon the interaction between independent variables. These figures may additionally indicate the effects of X_2 and X_4 on P_{CO_2}, α_{CO_2/CH_4}, α_{O_2/N_2}, and α_{N_2/CH_4} response. Fig. 7 shows the effects of nanoparticles and polymer content on CO_2 permeability. The addition of the nanoparticles to the membrane has increased the CO_2 permeability, since it is known as an effective factor improving the membrane permeability. On the other hand, adding polymer content in the membrane had a negative effect and reduced the amount of increment in the permeability. Therefore, the best status for the CO_2 permeability was obtained at low X_2 and high X_4. This behavior may be described by the membrane structure and the gas type. This indicates that an increment in the nanoparticle content of the nanoparticle and polymer composition has been found useful within the lim-

Table 7. The polynomial models obtained for the permeability and selectivity of various investigated gases using statistical significance check and multiple regression analysis

$P_{CH_4}=0.56+$	$P_{N_2}=0.69+$	$P_{O_2}=2.03+$	$\alpha_{N_2/CH_4}=1.17-$	$\alpha_{O_2/N_2}=3.25-$	$\alpha_{CO_2/N_2}=13.35-$
$0.091\times X_1$	$0.1\times X_1$	$0.088\times X_1$	$0.047\times X_1$	$0.21\times X_1$	$0.77\times X_1$
$-0.026\times X_2$	$-0.027\times X_2$	$-0.016\times X_2$	$-0.024\times X_2$	$-0.11\times X_2$	$-1.11\times X_2$
$+0.038\times X_3$	$+0.056\times X_3$	$+0.09\times X_3$	$+8.544E\text{-}03\times X_3$	$+0.62\times X_3$	$+1.98\times X_3$
$+0.17\times X_4$	$+0.24\times X_4$	$+0.19\times X_4$	$+0.016\times X_4$	$-0.16\times X_4$	$-0.62\times X_1X_3$
$+0.016\times X_1X_2$	$+0.02\times X_1X_2$	$+8.29E\text{-}04\times X_1X_2$	$-2.8E\text{-}03\times X_1X_2$	$-0.18\times X_1X_3$	$-0.7\times X_1X_4$
$+0.014\times X_1X_3$	$+0.018\times X_1X_3$	$-0.044\times X_1X_3$	$-0.011\times X_1X_3$	$-0.57\times X_2X_3$	$-0.98\times X_2X_3$
$+0.024\times X_1X_4$	$+0.028\times X_1X_4$	$+0.015\times X_1X_4$	$+0.033\times X_2X_3$	$+0.27\times X_2X_4$	$+0.49\times X_4^2$
$-0.018\times X_2X_3$	$-0.022\times X_2X_3$	$-0.034\times X_2X_3$	$+0.035\times X_4^2$	$-0.36\times X_1X_2X_4$	$+0.1\times X_1X_3X_4$
$+6.419E\text{-}04\times X_2X_4$	$+1.88E\text{-}03\times X_2X_4$	$+0.57\times X_3X_4$	$-0.013\times X_1X_2X_3$	$+0.26\times X_2X_3X_4$	$-0.47\times X_2X_3X_4$
$+6.737E\text{-}03\times X_3X_4$	$+0.019\times X_3X_4$	$+0.045\times X_1X_2X_3$	$+0.03\times X_1X_2X_4$	$+0.39\times X_2X_4^2$	$+0.66\times X_1X_4^2$
		$+0.068\times X_1X_2X_4$	$+0.021\times X_1X_3X_4$	$-0.74\times X_3X_4^2$	$+1.35\times X_3X_4^2$
		$-0.04\times X_2X_3X_4$	$-0.022\times X_2X_3X_4$		$-1.34\times X_3X_4^2$
			$+0.073\times X_1X_4^2$		$-0.15\times X_4^3$

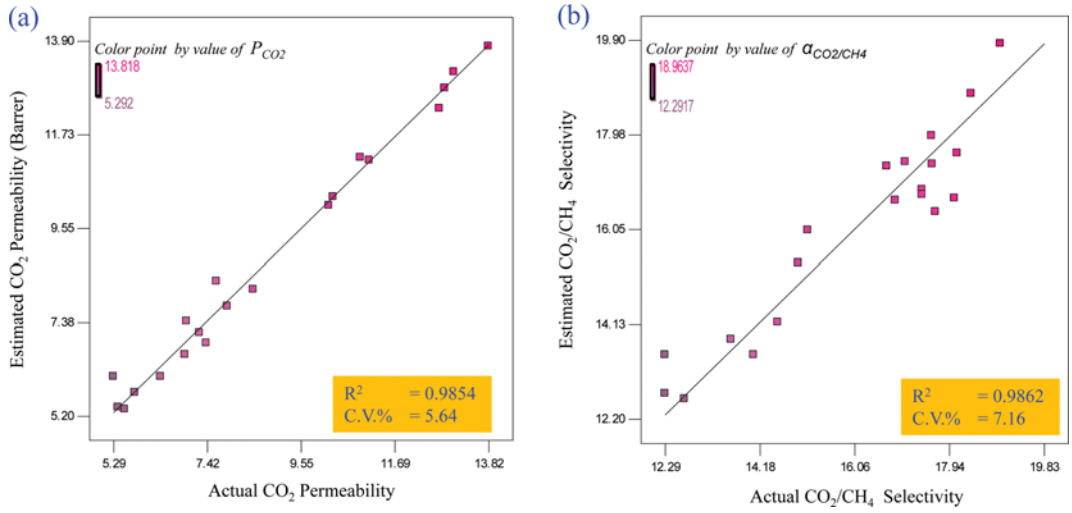

Fig. 6. Estimated (a) CO_2 permeability and (b) CO_2/CH_4 selectivity versus actual experimental data obtained at optimum conditions.

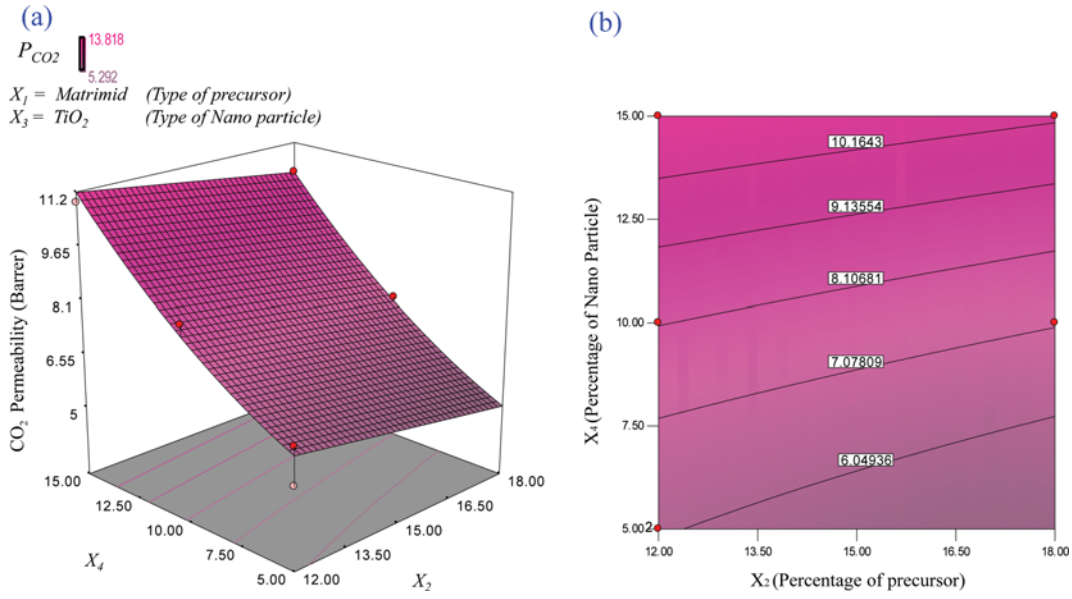

Fig. 7. The combined effects of percentage of nano-particle and precursor on the CO_2 permeability with average material (actual factor). (a) Surface plot and (b) contour plot.

itation range studied for gas permeability. This is while adverse results were achieved for the gas selectivity. For example, from Fig. 8, one can conclude that the increment of nanoparticles and polymer content will simultaneously improve the membrane efficiency and increase the CO_2/CH_4 selectivity that altogether implies compatibility between the polymer and the nanoparticles at high percentages. However, the combination of these two parameters in low percentages of the polymer will reduce the efficiency of the membrane in comparison to the previous status, and it would not show positive results. For example, in low X_2, an increment of X_4 will increase the selectivity at first. Consecutively, further addition of the nanoparticles to the membrane will reduce the selectivity. Selectivity results of CO_2/CH_4 and O_2/N_2 are shown in Figs. 8 and 9. As seen, these data exhibit a general increment in MMMs selectivities relative to enhance nanoparticle percentage. An apparent reduction in gas pair selectivities was detected in MMMs containing lower TiO_2 and SiO_2 nanoparticles, which may be related to formation of micron-size aggregates and unselective voids in mixed matrix and composite network. The MMMs have been practiced by integrating and containing typical fillers such as nanoparticles [41-45], multiwall carbon nanotubes [46], zeolites [47,48], metal organic framework (MOF) [49], graphene [50] as potential fillers in the polymer network. The gas separation performance of these matrix membranes depends considerably on the polymeric precursor and filler type in addition to the organic and inorganic interaction. Nanoparticles such as MgO, ZnO, SiO_2 and TiO_2 are high performance materials due to their potential applications for MMMs development technology. The nanoparticle contribution

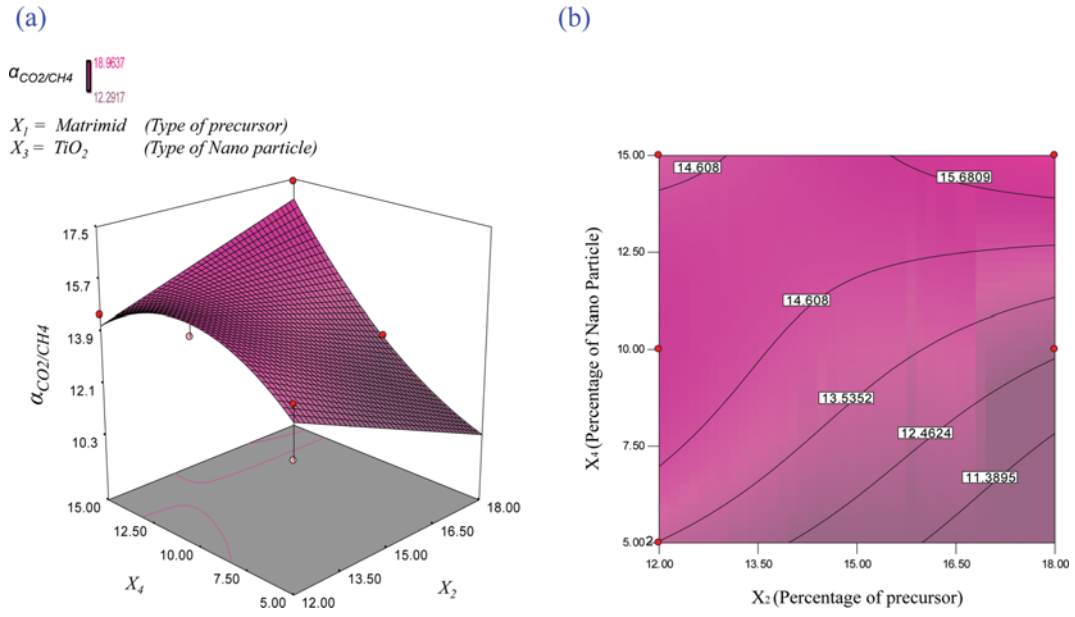

Fig. 8. The combined effects of percentage of nano-particle and precursor on the CO_2/CH_4 selectivity with average material (actual factor). (a) Surface plot and (b) contour plot.

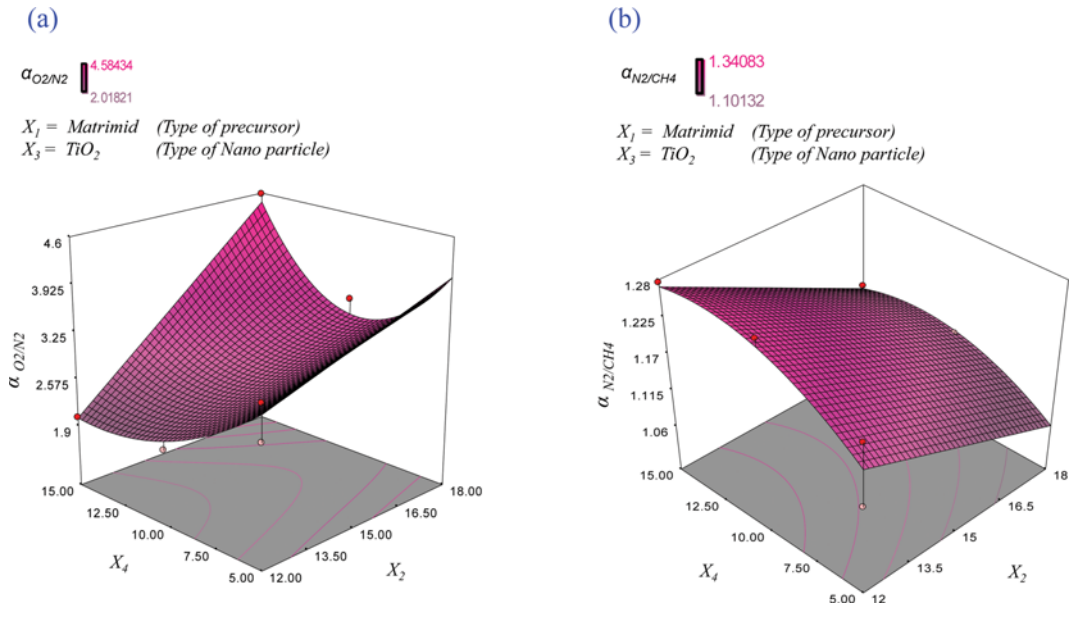

Fig. 9. Response surface plot on the (a) O_2/N_2 and (b) N_2/CH_4 selectivity of the combined effects of percentage of nano-particle and precursor.

in the appropriate preparation condition would result in significantly improved permeability while maintaining ideal selectivity. The gas transport results from MMMs comprised from various polymeric precursor and nanoparticles are summarized in Table 8. It is specified that the mixed matrix membranes made of PSF and SiO_2 have acceptable values of gas permeability than the usual ones. Furthermore, they have proper selectivity, which is more than the amount of gas pair selectivity in common polymeric membrane.

5. Adequacy Evaluation of Model

Basically, an appropriate model must be confirmed to provide a proper approximation for actual systems. Some evaluations have been fulfilled based on a regular hypothesis upon a normal probability plot (Fig. 10). Regular hypothesis has been in accordance with the remainder plot on a straight line. Fig. 11 depicts a drawing from the remaining amounts based on the approximate values. One of the important results is that the remaining amounts are randomly dispersed. It can also be proposed that the variance of the initial value is constant for all the results. Figs. 10 and 11 show that gas transport is both acceptable and satisfactory to describe the permeability and selectivity. The accuracy of all the models was also checked by various factors, including determination coefficient (R^2), coefficient of variation (CV) and correlation coefficient (R).

Table 8. Separation performance of prepared MMMs in comparison to other investigated MMMs

Conventional fillers	Type of polymer	Type of filler	Percentage of filler	Operating temperature (°C)	Operating pressure (bar)	Permeability (barrer)			Selectivity		Ref.
						P_{CO_2}	P_{CH_4}	P_{N_2}	α_{CO_2/CH_4}	α_{CO_2/N_2}	
Metal oxides	Matrimid	TiO_2	15	35	2	21.1	1.8		13.8		[38]
	ETPU	SiO_2	15	30	10	8.9	0.3		28.3		[39]
	BSPPOdp 8020	SiO_2	9	25	7.1	48		1.2		40	[40]
This work	Matrimid	TiO_2	15	25	8	10.3	0.57	0.73	18.1	14.09	
		SiO_2	15	25	8	11.1	0.59	0.79	18.96	14.14	
	Polysulfone	TiO_2	15	25	8	12.7	0.84	1.05	15.13	12.07	
		SiO_2	15	25	8	13.0	0.87	1.11	14.94	11.71	

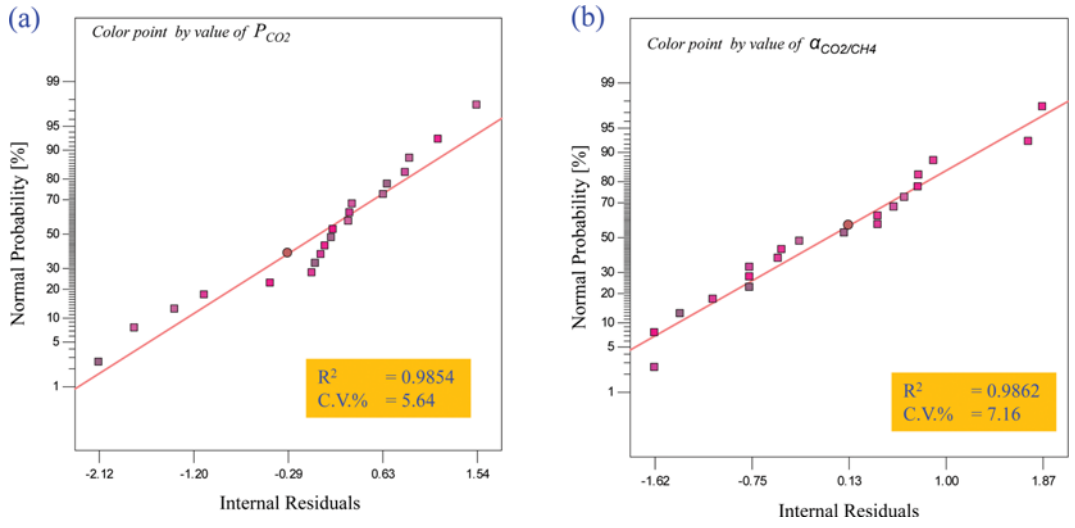

Fig. 10. The plots of normal probability vs. internal residuals for (a) CO_2 permeability and (b) CO_2/CH_4 selectivity of membranes.

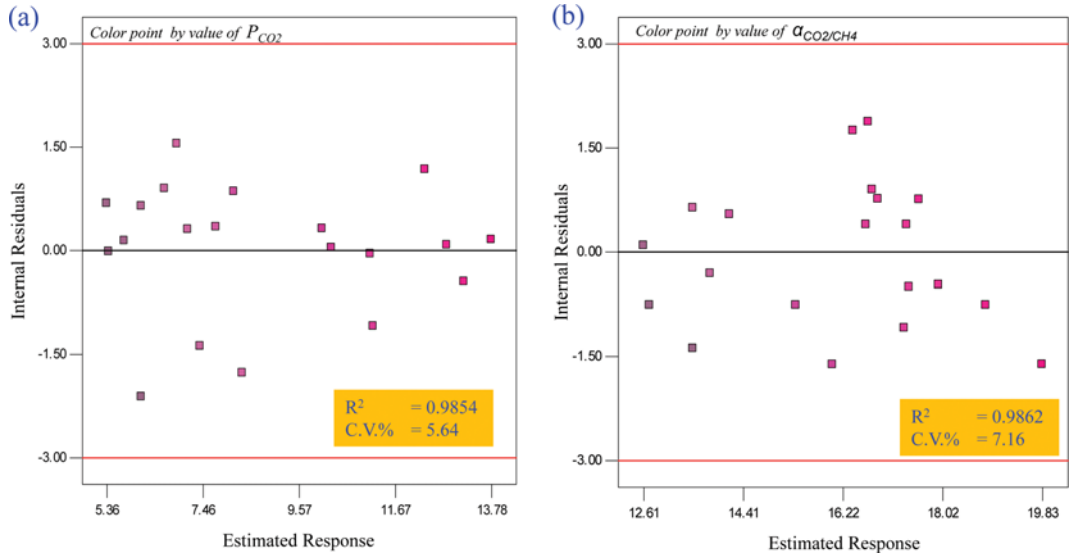

Fig. 11. The plots of internal residuals vs. estimated response for (a) CO_2 permeability and (b) CO_2/CH_4 selectivity of membranes.

R^2 value of each model suggests the variations of 98.44, 98.25, 92.19 and 98.54 for the permeability of CH_4, N_2, O_2 and CO_2, respectively, in addition to 92.66, 98.62, 92.83 and 97.74 for the selectivity of N_2/CH_4, CO_2/CH_4, O_2/N_2 and CO_2/N_2, respectively. Furthermore, a lower value of CV (6.12, 7.24, 6.17 and 5.64 for the permeability of CH_4, N_2, O_2 and CO_2, respectively, and also 2.89, 7.16, 11.35 and

Table 9. Minimum and maximum limits and set goal for each response to generate optimal conditions

Name	Goal	Lower Limit	Upper limit	Lower Weight	Upper Weight	Importance
Precursor material (X_1)	is in range	Matrimid	PS	1	1	3
Blend composition (X_2)	is in range	12	18	1	1	3
Pyrolysis temperature (X_3)	is in range	TiO_2	SiO_2	1	1	3
Pyrolysis vacuum pressure (X_4)	is in range	5	15	1	1	3
P_{CH_4}	maximize	0.314	0.951	3	1	3
P_{N_2}	maximize	0.353	1.213	2	1	3
P_{O_2}	maximize	1.57	2.45	2	1	3
P_{CO_2}	maximize	5.29	13.82	3	1	3
α_{N_2/CH_4}	maximize	1.10	1.34	4	1	4
α_{CO_2/CH_4}	maximize	12.29	18.96	5	1	5
α_{O_2/N_2}	maximize	2.02	4.58	4	1	4
α_{CO_2/N_2}	maximize	10.93	15.98	3	1	3

Table 10. Optimum process conditions and their results for validation of model

Number	X_1	X_2	X_3	X_4	P_{CH_4}	P_{N_2}	P_{O_2}	P_{CO_2}	α_{N_2/CH_4}	α_{CO_2/CH_4}	α_{O_2/N_2}	α_{CO_2/N_2}	Desirability
1	Matrimid	12	SiO_2	12.24	0.625	0.798	2.47	10.23	1.22	21.21	4.23	18.70	0.363
2	Matrimid	12	SiO_2	12.35	0.628	0.803	2.47	10.30	1.22	21.16	4.19	18.66	0.363
3	Matrimid	12	SiO_2	11.91	0.615	0.783	2.44	10.02	1.22	21.36	4.36	18.79	0.362
4	PS	12	SiO_2	13.82	0.885	1.113	2.49	12.82	1.21	17.68	3.24	14.97	0.294
5	PS	18	TiO_2	15	0.795	0.984	2.16	12.33	1.23	16.40	3.68	14.46	0.236
6	PS	12	SiO_2	7.61	0.642	0.757	2.19	8.67	1.14	17.57	4.06	15.76	0.112
7	PS	12	SiO_2	7.96	0.656	0.778	2.21	8.86	1.13	17.66	4.11	15.84	0.112
8	Matrimid	16.4	TiO_2	15	0.574	0.733	1.87	10.52	1.16	16.07	3.81	14.12	0.082
9	Matrimid	16.46	TiO_2	15	0.574	0.733	1.87	10.51	1.16	16.09	3.83	14.16	0.082
Repeat test	Matrimid	12	SiO_2	12.24	0.621	0.812	2.48	10.51	1.21	21.80	4.21	18.90	0.363
Error percent	×100				0.58	−1.73	−0.63	−2.77	1.16	−2.76	0.56	−1.07	

3.5 for the selectivity of N_2/CH_4, CO_2/CH_4, O_2/N_2 and CO_2/N_2, respectively) reported in the present study are referred to the reliability of the experiments and their superior accuracy as well.

6. Model Validation and Optimization

A proper model was selected for the performance results and responses of gas separation and gas transport for the purpose of optimization. Statistical optimization and submission of the optimal values of parameters and results can be carried out by maximizing and optimizing all models of selectivity and permeability. Table 9 lists the minimum and maximum limits and the value set for each response to generate optimal conditions. The optimized conditions as submitted in the first row of Table 10 indicate that the membrane was formed from Matrimid (12)/SiO_2 (12.24). In this table, the other improved conditions are shown for approximate values of the gas permeability and selectivity. A duplicate gas permeability experiment confirmed the improvement approach. An acceptable coordination between the experimental results and the approximate data can be noticed from the other results that may occur due to a slight variation in the experimental conditions. Based on the results of this table, the maximum gas permeability in the synthetic membrane of PSF (12)/SiO_2 (13.82) and the maximum selectivity of gases were observed in the membrane of Matrimid (12)/SiO_2 (11.91). The maximum value of permeability for the gases of CO_2, N_2, CH_4 and CO_2, was obtained as 2.49, 1.113, 0.885 and 12.82, respectively .The maximum value of selectivity for CO_2/CH_4, CO_2/N_2, O_2/N_2 and N_2/CH_4, was 21.36, 18.79, 4.36 and 1.23, respectively, for the mixed matrix membranes.

CONCLUSION

We investigated the effect of adding nanoparticles of TiO_2 and SiO_2 on the efficiency of polymer membranes, made of Matrimid® and Polysulfone, to investigate the effects of different parameters on the specifications of gas transport properties. Type of polymer, polymer content, type of nanoparticles and nanoparticles content were examined as the main controller parameters. Experimental designing, modeling and improving gas separation procedure were fulfilled. For this purpose, eight quadratic and cubic models wereen provided for the selectivity of CO_2/CH_4, CO_2/N_2, O_2/N_2 and N_2/CH_4 and also the permeability of O_2, N_2, CH_4 and CO_2. The model presented in this research shows that all the proposed equations are significant and can be used to improve the analysis. When there are nanoparticles in the polymer network, the permeability of the mixed matrix membrane increased in comparison to the pure

polymer due to compression of the polymer chains and larger free volume of the membrane network. Outputs from the optimization results revealed that the membrane of Matrimid (18)/SiO_2 (15) incorporated the maximum selectivity for CO_2/CH_4 and N_2/CH_4, while the maximum selectivity for O_2/N_2 and CO_2/N_2 was obtained in the synthetic membrane of Matrimid (12)/TiO_2 (5). On the other hand, the maximum gas permeability was achieved in high percentages of the nanoparticles and low percentages of the polymer. The synthetic network membrane of PSF (12)/SiO_2 (15) presented the best results for the gas permeability. Concentration of the polymer solution, conditions/manner of the membrane synthesis, improvement of the compatibility between the polymer and the nanoparticles may have significant effects on the membrane efficiency especially in great densities of the nanoparticles. The mixed matrix membrane developed in this study will be used for different applications of the gas industry.

NOMENCLATURE

PSF : polysulfone
CV : coefficient of variation
R : correlation coefficient
R^2 : coefficient of multiple determinations
R^2_{adj} : adjusted statistic coefficient
DOF : degree of freedom
F-value : ratio of variances, computed value
P-value : statistical criterion
Y : response
$\overline{X}$: mean value of variables
X_1, X_2, X_3 : coded variables
$b_0, b_1, \ldots, b_n$: regression coefficients
i and j : subscripts (integer variables)
n : number of factors (variables)

REFERENCES

1. M. A. Semsarzadeh, B. Ghalei, M. Fardi, M. Esmaeeli and E. Vakili, *Korean J. Chem. Eng.*, **31**, 841 (2014).
2. A. Jomekian, S. A. A. Mansoori, N. Monirimanesh and A. Shafiee, *Korean J. Chem. Eng.*, **28**, 2069 (2011).
3. F. S. Halek, S. K. Farahani and S. M. Hosseini, *Korean J. Chem. Eng.*, **33**, 629 (2016).
4. E. Bagheripour, A. Moghadassi and S. M. Hosseini, *Korean J. Chem. Eng.*, **33**, 1462 (2016).
5. N. Nabian, A. A. Ghoreyshi, A. Rahimpour and M. Shakeri, *Korean J. Chem. Eng.*, **32**, 2204 (2015).
6. G.-L. Zhuang, M.-Y. Wey and H.-H. Tseng, *Chem. Eng. Res. Design*, **104**, 319 (2015).
7. V. Pirouzfar, S. S. Hosseini, M. R. Omidkhah and A. Z. Moghaddam, *Polym. Eng. Sci.*, **54**(1), 147 (2014).
8. S. S. Hosseini, M. R. Omidkhah, A. Z. Moghaddam, V. Pirouzfar, W. B. Krantz and N. R. Tan, *J. Sep. Purif.*, **122**, 278 (2014).
9. A. K. Zulhairun, A. F. Ismail, T. Matsuura, M. S. Abdullah and A. Mustafa, *Chem. Eng. J.*, **241**, 495 (2014).
10. D. L. Kuehne and S. K. Friedlander, *Ind. Eng. Chem. Proc. Des. Dev.*, **19**, 609 (1980).
11. H. B. Park, J. K. Kim, S. Y. Nam and Y. M. Lee, *J. Membr. Sci.*, **220**, 59 (2003).
12. T. C. Merkel, Z. He, I. Pinnau, B. D. Freeman, P. Meakin and A. J. Hill, *Macromolecules*, **36**, 6844 (2003).
13. P. M. Budd, K. J. Msayib, C. E. Tattershall, B. S. Ghanem, K. J. Reynolds, N. B. McKeown and D. Fritsch, *J. Membr. Sci.*, **251**, 263 (2005).
14. M. Niwa, H. Kawakami, T. Kanamori, T. Shinbo, A. Kaito and S. Nagaoka, *Macromolecules*, **34**(26), 9039 (2001).
15. I. Soroko and A. Livingston, *J. Membr. Sci.*, **343**(1-2), 189 (2009).
16. L. Diestel, N. Wang, A. Schulz, F. Steinbach and J. Caro, *Ind. Eng. Chem. Res.*, **54**(3), 1103 (2015).
17. M. Heuchel and D. Hofmann, *Desalination*, **144**(1-3), 67 (2002).
18. S. Frimpong, C. A. Plank and W. L. S. Laukhuf, *Chem. Eng. J.*, **47**(2), 63 (1991).
19. H. J. Song, Y. J. Jo, S.-Y. Kim, J. Lee and C. K. Kim, *J. Membr. Sci.*, **466**, 173 (2014).
20. A. Mollahosseini, A. Rahimpour, M. Jahamshahi, M. Peyravi and M. Khavarpour, *Desalination*, **306**, 41 (2012).
21. S. Kim and E. Marand, *Micropor. Mesopor. Mater.*, **114**(1-3), 129 (2008).
22. M. Rabbani Esfahani, J. L. Tyler, H. A. Stretz amd M. J. M. Wells, *Desalination*, **372**, 47 (2015).
23. J. Ahn, W. J. Chung, I. Pinnau and M. D. Guiver, *J. Membr. Sci.*, **314**, 123 (2008).
24. T. C. Merkel, Z. He, I. Pinnau, B. D. Freeman, P. Meakin and A. J. Hill, *Macromolecules*, **36**, 8406 (2003).
25. T. C. Merkel, B. D. Freeman, R. J. Spontak, Z. He, I. Pinnau, P. Meakin and A. J. Hill, *Science*, **296**, 519 (2002).
26. S. Matteucci, V. A. Kusuma, S. Swinnea and B. D. Freeman, *Polymer*, **49**, 757 (2008).
27. F. Moghadam, M. R. Omidkhah, E. V. Farahani, M. Z. Pedram and F. Dorosti, *Sep. Purif. Technol.*, **77**, 128 (2011).
28. X. Duthie, S. Kentish, C. Powell, K. Nagai, G. Qiao and G. Stevens, *J. Membr. Sci.*, **294**, 40 (2007).
29. V. Pirouzfar, M. Mosalmani and M. Mortezaei, *Iranian Polymer J.*, **24**(10), 829 (2015).
30. C. J. Anderson, S. J. Pas, G. Arora, S. E. Kentish, A. J. Hill, S. I. Sandler and G. Stevens, *J. Membr. Sci.*, **322**, 19 (2008).
31. M. Azeman, A. Madzlan, I. A. Fauzi, H. Hasrinah, S. Suhaila and H. Abdul Rahman, Development of asymmetric carbon hollow fiber membrane for gas separation, Project Report, Universiti Teknologi Malaysia (2006).
32. M. Khayet, C. Cojocaru and M. C. Garcia-Payo, *J. Membr. Sci.*, **351**, 234 (2010).
33. P. Onsekizoglu, K. Savas Bahceci and J. Acar, *J. Membr. Sci.*, **349**, 225 (2010).
34. Jincai Su and Aik Chong Lua, *J. Membr. Sci.*, **278**, 335 (2006).
35. V. Pirouzfar, S. S. Hosseini, M. R. Omidkhah and A. Z. Moghaddam, *J. Ind. Eng. Chem. Res.*, **40**(3), 1061 (2014).
36. Standard test methods for specific gravity (relative density) and density of plastics by displacements. ASTM annual book of standards; 1993. D-792.
37. A. Bondi, *J. Phys. Chem.*, **68**, 441 (1964).
38. A. C. Lua and J. Su, *Carbon*, **44**, 2964 (2006).
39. P. S. Tin, T.-S. Chung, Y. Liu and R. Wang, *Carbon*, **42**, 3123 (2004).

40. S. S. Hosseini and T. S. Chung, *J. Membr. Sci.*, **328**, 174 (2009).
41. A. Kılıç, Ç. Atalay-Oral, A. Sirkecioğlu, Ş. Birgül Tantekin-Ersolmaz and M. Göktuğ Ahunbay, *J, Membr. Sci.*, **489**, 81 (2015).
42. L. Ge, Z. Zhu, F. Li, S. Liu, L. Wang, X. Tang and V. Rudolph, *J. Phys. Chem. C.*, **115**, 6661 (2011).
43. S. N. Wijenayake, N. P. Panapitiya, S. H. Versteeg, C. N. Nguyen, S. Goel, K. J. Balkus Jr., I. H. Musselman and J. P. Ferraris, *Ind. Eng. Chem. Res.*, **52**, 6991 (2013).
44. M. H. Nematollahi, A. H. Saeedi Dehaghani and R. Abedini, *Korean J. Chem. Eng.*, **33**(2), 657 (2016).
45. M. H. Nematollahi, A. H. Saeedi Dehaghani, V. Pirouzfar and E. Akhondi, *Macromole. Res.*, **24**, Issue 9, 782 (2016).
46. S. F. Soleymanipour, A. H. Saeedi Dehaghani, V. Pirouzfar and A. Alihosseini, *J. Appl. Polym. Sci.* (2016), DOI:10.1002/app.43839.
47. M. Pakizeh, S. Ofoghi and S. H. R. Shooshtari, *Korean J. Chem. Eng.* (2016), DOI:10.1007/s11814-016-0166-7.
48. J. H. Moon, H. Ahn, S. H. Hyun and C. H. Lee, *Korean J. Chem. Eng.*, **21**, 477 (2004).
49. M. Arjmandi, M. Pakizeh and O. Pirouzram, *Korean J. Chem. Eng.*, **32**, 1178 (2015).
50. M. Moochani, A. Moghadassi, S. M. Hosseini, E. Bagheripour and F. Parvizian, *Korean J. Chem. Eng.*, **33**, 2674 (2016).